JOURNAL OF SOLID STATE CHEMISTRY 15, 24–39 (1975)

# Phase Transitions in Tungsten Trioxide at Low Temperatures

I. LEFKOWITZ,* M. B. DOWELL,† AND M. A. SHIELDS

*Pitman-Dunn Laboratory, Frankford Arsenal, Philadelphia, Pennsylvania 19137*

Received September 27, 1974

Capacitance and electrical resistivity measurements have been made on stoichiometric and on oxygen-deficient tungsten trioxide crystals from 4.2 to 300°K. X ray oscillation and rotation photographs were made on single crystals of both materials near 200°K and near 300°K. Capacitance and resistivity anomalies identify phase transitions near 40, 65, 130, 220, and 260°K in stoichiometric $WO_3$. Resistivity anomalies occur near 80, 130, 220, and 260°K in oxygen-deficient tungsten trioxide. Capacitance measurements suggest that the transformation at 130°K of a low-temperature phase to a high-temperature phase of stoichiometric $WO_3$ is associated with a doubling of the *c*-parameter of the unit cell. Resistivity measurements establish probable conduction mechanisms in each phase of stoichiometric and of oxygen-deficient tungsten trioxide, and show that oxygen-deficient tungsten trioxide undergoes a semiconductor-to-metal transition near 220°K. Electronic phenomena that do not appear to be associated with structural phase transformations are observed near 16°K in stoichiometric $WO_3$.

## 1. Introduction

Studies of the properties of tungsten trioxide have attracted attention because of the large number of phases observed at elevated temperatures (*1*) and because of reports of ferroelectricity (*2, 3*) and of antiferroelectricity (*4*) in some of these phases. Other studies have demonstrated the existence of a number of low-temperature phases: (a) ferroelectric hysteresis loops have been observed at 77°K (*5*); (b) electrical transport studies on single crystals have identified a piezoelectric phase occurring from 250 to 287°K in which the conduction electrons are predominantly scattered by acoustical phonons, and a phase occurring below 250°K in which an observed large phonon drag effect would be consistent with either a ferroelectric or an antiferroelectric crystal structure (*6*). Such observations may have a direct bearing on current theories of ferroelectricity and of antiferroelectricity, since the occurrence of these phenomena in two-element compounds is rather rare (*7–9*). Dispersion curve measurements of such a system could provide a better understanding of ferroelectric phenomena (*10–12*).

Phase transitions in tungsten trioxide often are associated with distortions of the oxygen octahedra that surround the heavy W atoms, and with changes in unit cell multiplicity (*1, 13, 14*). Similar cell-multiplicity changes are associated with transformations from ferroelectric to antiferroelectric phases in sodium niobate (*15, 16*). These octahedral distortions have profound effects on the domain structure (*13*), lattice polarizability (*17*) and, probably, on the electron band structure (*6*). Capacitance and electrical resistivity studies of tungsten trioxide might be expected to reveal phase transitions that might not be readily observable by other means.

Capacitance and electrical resistivity measurements obtained in the same range of temperature can provide rather complete information concerning the phase transitions. Large single crystals having suitable domain

* Present address: Princeton Materials Science, Princeton, New Jersey 08540.

† Present address: Parma Technical Center, Union Carbide Corporation, Cleveland, Ohio 44101.

orientations can be prepared (*17–20*). Ordered shear structures corresponding to compositions $WO_{3-x}$ ($0 \leqslant x \leqslant 0.02$) can be prepared by suitable reduction of these single crystals (*21–24*). Rather subtle changes in stoichiometry and in crystal structure might be expected to produce noteworthy changes in the electrical properties of this material. Dielectric and electron transport measurements have been shown to be especially well-adapted to the study of phase transitions in substoichiometric transition metal oxides having ordered shear structures (*25*).

## 2. Preparation of Single Crystals

Chemically pure tungsten trioxide powder was obtained from Sylvania Chemicals as 99.5% pure Type TO-1. A typical assay (Schwartzkopf Microanalytical Laboratories, New York) reported 79.02wt %W (theoretical: 79.29%), while semiquantitative emission spectra and trace element analyses showed 0.15% Na and less than 0.01% Mg. No other impurity was detected; limits of detectability of these emission spectra vary from 0.6% for Ta to 0.003% for Ag and Cu. Different lots of powder gave closely similar results. Trace element analyses of single crystals of stoichiometric and oxygen-deficient tungsten trioxide are reported below.

Single crystals of stoichiometric $WO_3$ were produced by sublimation in a thermal gradient. A 1.6-cm diameter Pt tube, sealed at one end, was charged with several grams of $WO_3$ powder. The charged and sealed end of the tube was heated to 1350°C for 20–30 hr in a tube furnace equipped with $MoSi_2$ heating elements, during which time single crystals grew in cooler portions of the tube. Crystals produced in this manner are wedge-shaped and have rectangular (001) growth faces as large as $0.5 \times 0.5$ cm. These crystals can be cleaved to produce (001) faces as large as 25 $mm^2$ and (111) faces as large as 10 $mm^2$. The color of stoichiometric $WO_3$ crystals grown in this manner varies with increasing thickness from dark yellow to olive green. Metallographic examination of (001) growth faces reveals hillocks similar to those observed previously (*1*, *14*, *17*). The growth spirals sometimes observed on crystal surfaces prepared in a different manner (*26*) were not observed during this investigation. All crystals used in this investigation exhibited parallel extinction when viewed between crossed polarizers, and all domains were parallel or near-parallel to adjacent domains. Conoscopic interference patterns showed the expected uniaxial positive birefringence at room temperature (*17*). Semiquantitative emission spectra of crystals produced in this manner showed about 0.03% Fe and Cu, 0.01% Ni, and less than 0.01% Mg. Fe, Cu, and Ni are common impurities in refined Pt. Comparison of vapor transpiration data for $WO_3$ in dry air (*27*) with that for $PtO_2$, which is formed by oxidation of Pt metal in air at 1350°C (*28*, *29*), indicates that the net rate of vapor transport of $PtO_2$ is about 0.1% of that of $WO_3$ at this temperature. No Pt was detected, however, at a detectability limit of 0.005%.

Single-crystal oscillation and full rotation X ray diffraction patterns were taken with the *c*-axis as the axis of rotation for a stoichiometric $WO_3$ crystal. The crystal was carefully selected to minimize twinning, but repeated temperature cycling invariably introduced some new domains. Photographs were taken both at room temperature and in the interval 203–223°K (Fig. 1). The repeat distance is 3.85 Å at room temperature and 7.7 Å in the interval 203–223°K. These results indicate that there is a change of periodicity along the *c*-axis in stoichiometric $WO_3$ prepared in the manner described above, which is associated either with the phase change which appears on cooling below about 260°K, or with that which appears on cooling below about 220°K. The repeat distance in the reduced oxide (*vide infra*) is already 7.7 Å at room temperature.

Single crystals of $WO_3$ obtained from the melt have given X ray diffraction patterns corresponding to the space group $P2_1/a$, $Z = 4$, $c = 3.84$ Å (*30–32*). Single crystals prepared by decomposition of $H_2WO_4$ and sequent heating of $WO_3$ powder to 1300°C in a quartz tube, however, give odd-order layer lines corresponding to $P2_1/n$, $Z = 8$, $c = 7.68$ Å (*14*). This result has been found for

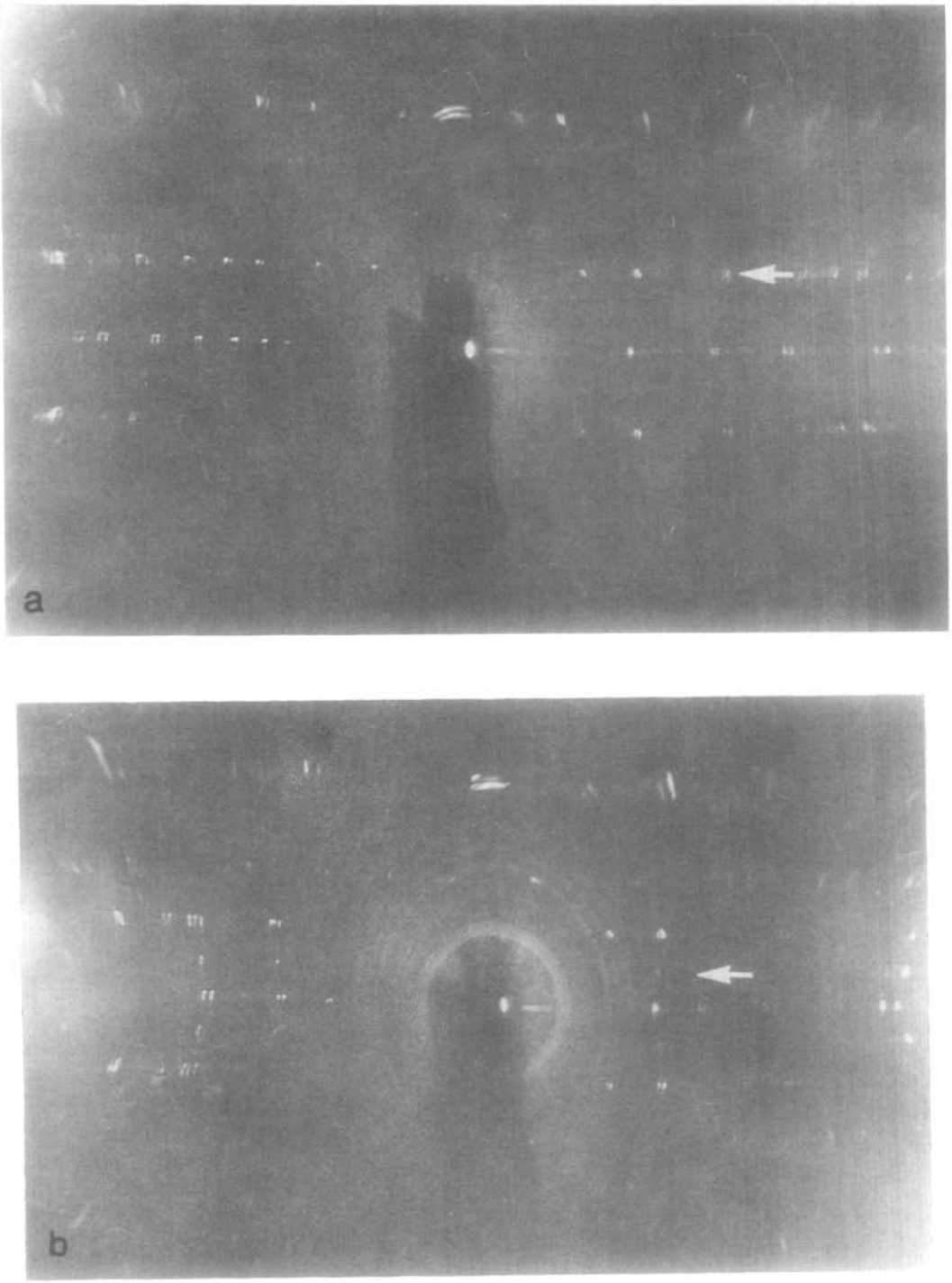


FIG. 1. (a) The diffraction pattern for $WO_3$ oscillated around the $c$-axis over an 11° arc at room temperature (301°K). (b) The same crystal, photographed after (a) as the temperature rose from 203 to 223°K. Arrows indicate the layer lines corresponding to 3.85 Å and 7.7 Å repeat distances.

single crystals grown by sublimation at 1300–1350°C in sealed Pt crucibles (*14*, *20*, *22*, *23*) and by recrystallization of $WO_3$ powder at 900°C in an $O_2$ atmosphere (*33*). Single crystals grown in sealed Pt crucibles exhibit additional diffraction lines corresponding to a triclinic pseudomonoclinic structure unless carefully annealed at 900°C for several hours (*20*), and it has been suggested that quantitative differences between electron transport properties of $WO_3$ single crystals grown on the powder charge and those grown on the Pt wall of the crucible may be due to subtle crystallographic differences between the two types of crystals (*19*). It seems likely that different procedures produce stoichiometric $WO_3$ crystals with slightly different room-temperature structures. Values of the repeat distance along the *c*-axis of stoichiometric $WO_3$ obtained by different investigations are given in Table I.

Tungsten trioxide single crystals were rendered oxygen-deficient by heating them in quartz boats while maintaining a vacuum of $10^{-5}$ Torr for several hours. Well-formed single crystals heated at 1090°K for 36 hr are dark green in color and do not differ in gross morphology from stoichiometric $WO_3$. The composition, determined by heating at 600°C in air until constant weight had been attained and the color had returned to that of the stoichiometric oxide, was $WO_{2.996}$. Microscopic examination in polarized transmitted light reveals two dark-line patterns, evidently consisting of planes parallel to the *c*-axis emerging on the (001) face, which intersect in a parallelogram pattern. The (001) face is thus divided into an array of domains showing essentially the same fourfold extinction. Optical (*22*, *23*), X ray (*22–24*), and electron micrographic (*24*) studies of oxygen-deficient tungsten trioxide crystals prepared in a fashion similar to that employed here have shown that this intersecting pattern is caused by clustering of oxygen vacancies to produce crystallographic shear along {120} planes. Well-formed $WO_3$ single crystals heated at 1370°K for 8 hr showed no gross morphological change from stoichiometric $WO_3$. These crystals were dark blue and were nearly opaque. The composition was $WO_{2.995}$. Microscopic examination of thin sections in transmitted light revealed a planar defect pattern similar to, but denser than, that reported above, while metallographic observations using polarized reflected light established that all parts of the surface showed the same extinction.

Single-crystal oscillation and full-rotation X ray diffraction patterns were taken along the *c*-axis of a well-formed oxygen-deficient tungsten trioxide crystal. Photographs were taken both at room temperature and at 193°K (Fig. 2). The repeat distance is 7.7 Å both in the room-temperature and in the low-temperature material. This result shows that, at room temperature, the repeat distance in the *c* direction of oxygen-deficient tungsten trioxide is twice that in the stoichiometric $WO_3$ single crystals grown in this investigation. From single crystal rotation photographs from crystals of compositions $WO_{2.9991}$ and $WO_{2.9881}$, Berak and Sienko (*22*, *23*) found a *C*-axis repeat distance of 7.71 Å. Semiquantitative emission spectrographic analysis of oxygen-deficient tungsten trioxide crystals used in this work showed essentially the same impurities as stoichiometric $WO_3$ crystals. However, spectrographic tests for Si are not particularly sensitive in the presence of large amounts of tungsten.

TABLE I

REPORTED SYMMETRIES AND *C*-AXIS REPEAT DISTANCES OF STOICHIOMETRIC $WO_3$ CRYSTALS IN VARIOUS INVESTIGATIONS

| Symmetry | *C*-axis repeat distance (Å) | Reference |
|---|---|---|
| Triclinic | 3.82 | (*34*) |
| Orthorhombic | 3.838 | (*30*) |
| Monoclinic | 3.824 | (*31*) |
| Monoclinic | 3.835 | (*32*) |
| Monoclinic | 3.84 | (*35*) |
| Monoclinic | 7.68 | (*14*) |
| Monoclinic | 7.688 | (*33*) |
| Monoclinic | 7.68 | (*21*) |
| Monoclinic | 3.83 | (*36*) |
| Monoclinic | 7.68 | (*20*) |
| Monoclinic | 7.71 | (*22*, *23*) |
| Monoclinic | 3.85 | This work |

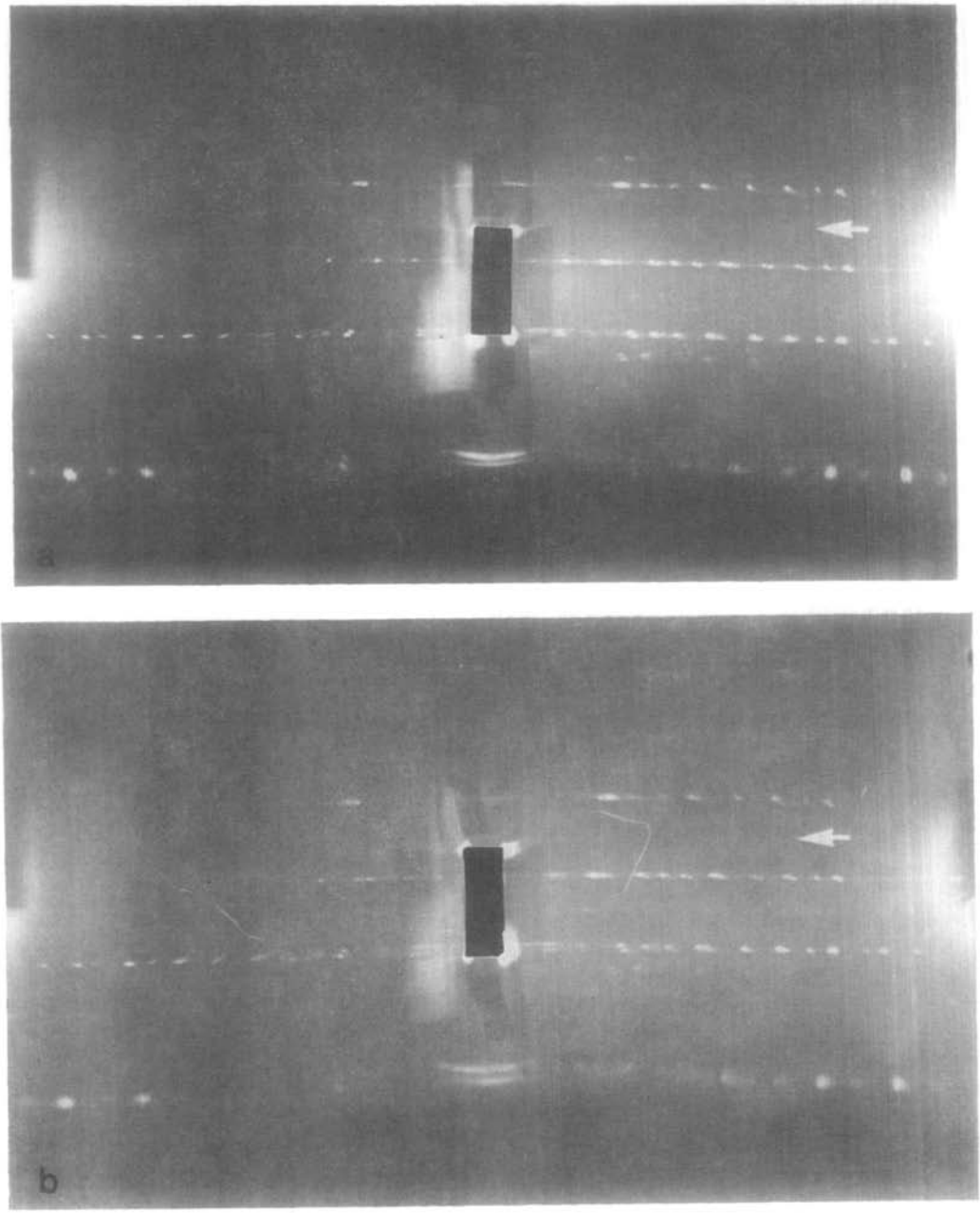


FIG. 2. (a) The diffraction pattern for oxygen-deficient tungsten trioxide at room temperature (301°K), oscillated over an 18° arc. (b) The pattern obtained at 193°K. Arrows indicate the layer lines corresponding to 7.7 Å repeat distances in both pictures.

Stoichiometric $WO_3$ powder pellets were cold-pressed under a pressure of 1.25 kbar in steel dies and sintered in air at 1270°K for 12 hr. Sintered wafers used for capacitance measurements were typically 2 cm in diameter and 0.32 cm thick.

## 3. Experimental Techniques

X ray diffraction patterns were obtained using a Norelco X ray diffraction unit equipped with a Nonius oscillation camera. Ni-filtered Cu$K\alpha$ radiation was employed. Crystal temperature was maintained by blowing a stream of dry nitrogen across the crystal; the nitrogen gas was passed through copper refrigerator tubing immersed in a liquid nitrogen bath, and flow rates were adjusted to maintain the desired crystal temperature. Temperature was measured using a chromel–alumel thermocouple junction affixed to the goniometer.

Capacitance and dielectric loss measurements on stoichiometric $WO_3$ single crystals and pressed pellets were made using a General Radio Type 1615-A three-terminal bridge operating at 1 kHz. Known areas on top and bottom surfaces of the sample were coated with Elmet LS232 liquid solder, and a margin around the edges of the sample was left uncoated. The *fringe* contribution to capacitance was estimated by measuring the capacitance of glass plates of known dielectric constant having the same size and shape as these samples. Fringe contributions were negligible except during measurements on the (111) faces of small crystals: fringing corrections were made to the capacitance measurements in these cases. Attempts to measure saturation polarizability of these samples were made using a modified Sawyer–Tower dielectric hysteresis loop tracer circuit. Measurements were made at frequencies of 60, 600, and 6000 Hz. Although the maximum field that can be obtained is limited by sample thickness, electric fields as large as 100 kV/cm could be obtained using thin samples.

Electrical resistance measurements were made using a Hickock Model DP 170 digital ohmmeter or a Kiethley Model 503 ac milliohmmeter, both operating in a four-terminal configuration. Electric currents in these circuits are sufficiently small that no heating of the sample was encountered. Resistivity measurements on oxygen-deficient tungsten trioxide crystals were made by the four-point potential probe method using sharpened steel wires as probes. Probe spacings were typically 1–2 mm and were measured using a calibrated optical comparator. Resistivity measurements on stoichiometric $WO_3$ single crystals were made by the bulk-volume resistivity method, since the pressure of spring-loaded contacts often causes crystals to fracture as they undergo displacive transitions. Known areas on (001) faces of these crystals were coated with Elmet liquid solder, to which current and voltage leads were attached without pressure. Extremely large resistivity values encountered during measurements on stoichiometric $WO_3$ single crystals at low temperatures were determined using a megohmmeter. Mutual inductance measurements on stoichiometric $WO_3$ powders were made using a Daunt mutual inductance bridge (*37*). The inductance sample was contained in an oxygen-free, high-conductivity copper sample holder.

Crystals used for electrical measurements were secured in a hollow space between the two halves of a demountable Teflon sample holder. Appropriate electrical connections extend from the crystal to brass terminals anchored in the Teflon block. These connections were made using a tin–indium solder that minimized thermal EMF. A similar sample arrangement (but in a three-terminal configuration) was used for capacitance measurements. The sample holder was wrapped in alternate layers of aluminum foil and Teflon tape to provide a large thermal mass and to minimize thermal gradients within the sample chamber. The sample chamber was attached to a thermally insulating rod that was raised and lowered in a helium cryostat. Rates of heating and cooling were typically 0.5–2.0°/min; slower rates were employed in temperature intervals in which earlier measurements had indicated the occurrence of phase transitions.

Low temperatures were obtained by lowering the sample probe into a standard wide-necked liquid nitrogen or liquid helium storage dewar. Temperatures were measured using a chromel–alumel thermocouple calibrated against liquid helium, liquid nitrogen, and ice water. The thermocouple junction was placed adjacent to the crystal in the sample holder. Temperature measurements are be-

lieved accurate to within ±2° from 30 to 300°K. A temperature of 4.2°K could be achieved by immersing the sample chamber in liquid helium. Temperatures in the range 4.2–30°K could be obtained by raising the sample chamber just above the He meniscus, allowing the liquid helium to drain, and taking measurements as the sample warmed.

## 4. Results

### *A. Stoichiometric $WO_3$*

Changes of dielectric constants ($\varepsilon$) and dissipation factors ($\tan\delta$) of 20 stoichiometric single crystals were measured as the temperature was cycled betwen 300 and 4.2°K. Plots of $\varepsilon$ and $\tan\delta$ measured in the *c* direction on one such crystal are given in Fig. 3, where capacitance anomalies are observed near 170 and 130°K, and $\tan\delta$ anomalies are observed near 130 and 65°K. Capacitance anomalies near these temperatures are also observed during measurements on (111) faces of small surface area. Measurements on these small faces are subject to the fringing effects discussed previously. The dielectric constant measured in the *c* direction changes little with temperature from 4.2 to 130°K, although a very small capacitance anomaly occurs near 65°K. Typical plots of $\varepsilon$ and $\tan\delta$ measured on sintered $WO_3$ pellets in the temperature range 4.2–300°K are shown in Fig. 4. Anomalies occur both in $\varepsilon$ and in $\tan\delta$ near 260, 220, 130, and 65°K. A small change in $\varepsilon$ and a large change in $\tan\delta$ are seen near 40°K. These anomalies near 200°K appear to be associated with a displacive transition from a high-temperature triclinic phase to a

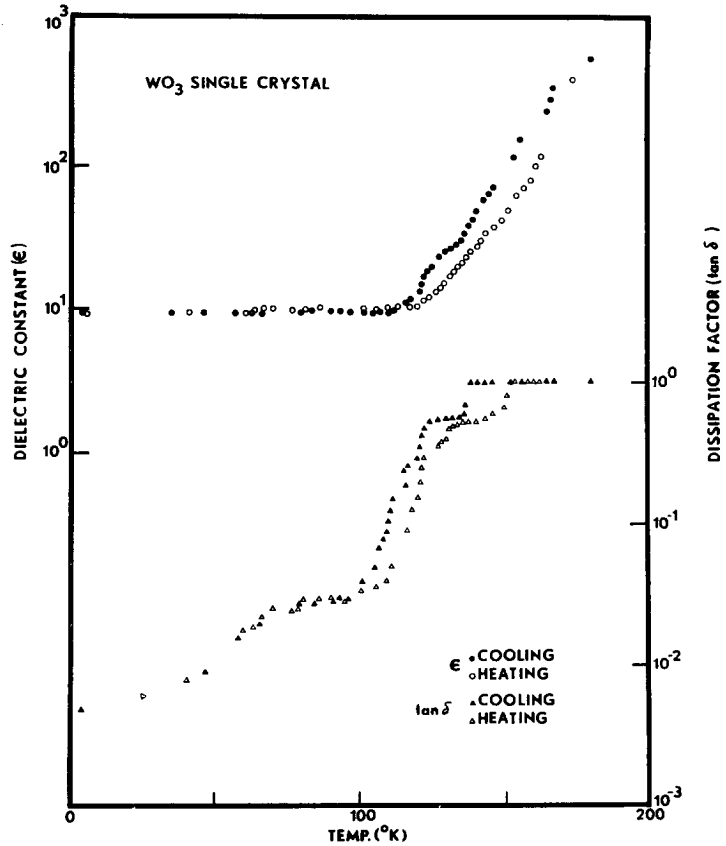


FIG. 3. Capacitance as a function of temperature, measured between nominal room-temperature (001) surfaces of a stoichiometric $WO_3$ single crystal at 1kHz.

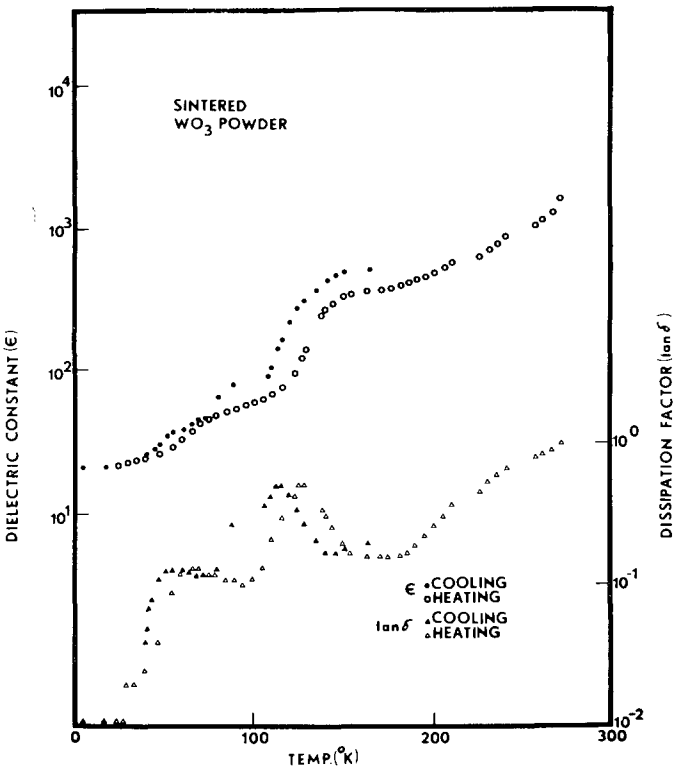


FIG. 4. Capacitance as a function of temperature, measured on sintered wafers of stoichiometric $WO_3$ powder at 1 kHz. Dielectric anomalies occur near 260, 220, 130, 65, and 40°K. *A* tan $\delta$ maximum occurs near 130°K.

low-temperature monoclinic (or possibly triclinic) phase (*14*); the diffraction photograph in Fig. 1b shows the 7.7 Å repeat distance of this low-temperature phase. The capacitance anomalies associated with this transition are subject to large thermal hystersis effects, as are changes in optical axis orientation and domain structure (*13*), in electrical resistivity and thermoelectric power (*6*, *22*, *23*), and in heat capacity (*38*).

Thermal hysteresis effects are also associated with the capacitance anomaly that occurs near 130°K. Single crystals frequently crack at this temperature, apparently because the volume of the crystal changes discontinuously.

The dielectric constant of sintered $WO_3$ pellets increases continuously as the temperature is increased from 30 to 300°K; no capacitance maximum or minimum is associated with the anomalies noted above. The dielectric constant is independent of temperature in the interval 4.2–30°K. Tan $\delta$ increases continuously as the temperature is increased from 210 to 300°K. A tan $\delta$ maximum occurs at 130°K. Tan $\delta$ is almost independent of temperature in the intervals 4.2–30°K, 70–110°K, and 150–210°K, but changes abruptly at the capacitance anomalies identified above.

Attempts were made to establish the existence of ferroelectric hysteresis loops in measurements on stoichiometric single crystals at 77 and 4.2°K. Measurements were made on several single crystals in three orthogonal directions using fields as high as 100 kV/cm, but no hysteresis loops were observed. Squarish hysteresis loops were occasionally observed in measurements made on sintered $WO_3$ pellets. These loops did not indicate complete saturation polarization and are therefore suspect.

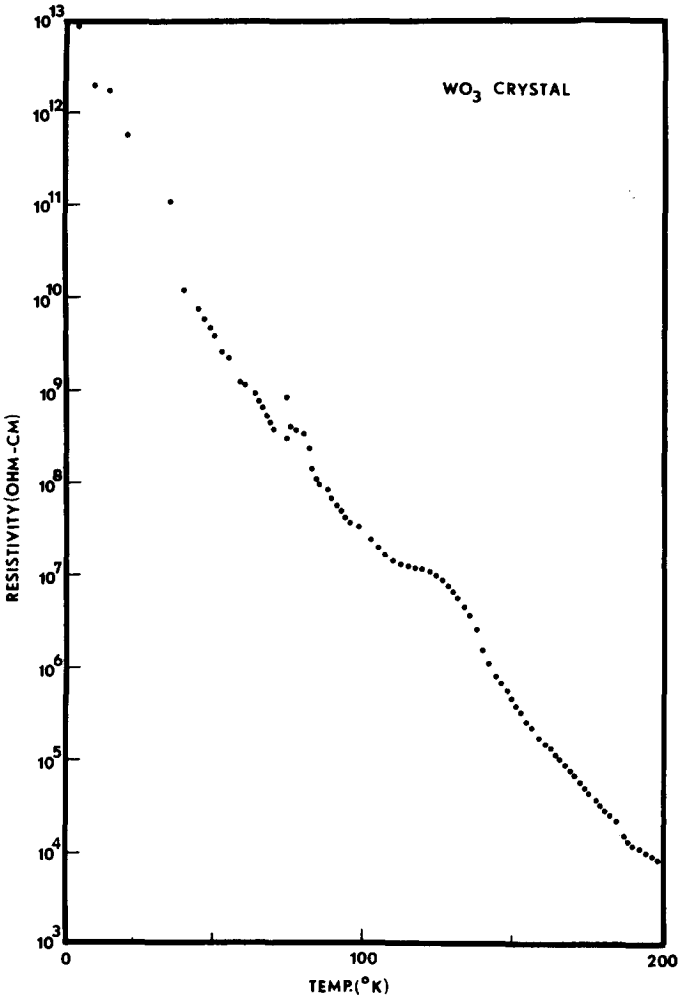


FIG. 5. The dc resistivity of a multidomain crystal of stoichiometric $WO_3$. Anomalies occur near 185, 130, 70 and 40°K. Measurements taken during cooling.

Bulk volume resistivity measurements between (001) faces of a typical stoichiometric $WO_3$ single crystal were made in the temperature interval 200–4.2°K (Fig. 5). Resistivity increases monotonically with decreasing temperature in the manner typical of nondegenerate semiconductors. Resistivity anomalies are observed near 185, 130, 70, and 40°K. These anomalies appear to correspond to the capacitance anomalies noted above; in particular, the anomaly at 185°K appears to be within the normal thermal hysteresis range of the capacitance anomaly at 220°K reported above. The crystals used in this study were selected to minimize twinning

TABLE II

ACTIVATION ENERGY FOR CONDUCTION OF STOICHIOMETRIC $WO_3$ SINGLE CRYSTALS IN VARIOUS TEMPERATURE INTERVALS

| Temperature interval (°K) | | |
|---|---|---|
| Upper limit | Lower limit | $\Delta E$ (eV) |
| 260 | 187 | 0.10 |
| 185 | 140 | 0.19 |
| 110 | 81 | 0.052 |
| 68 | 38 | 0.028 |
| 34 | 14 | 0.006 |
| 14 | 4.2 | — |

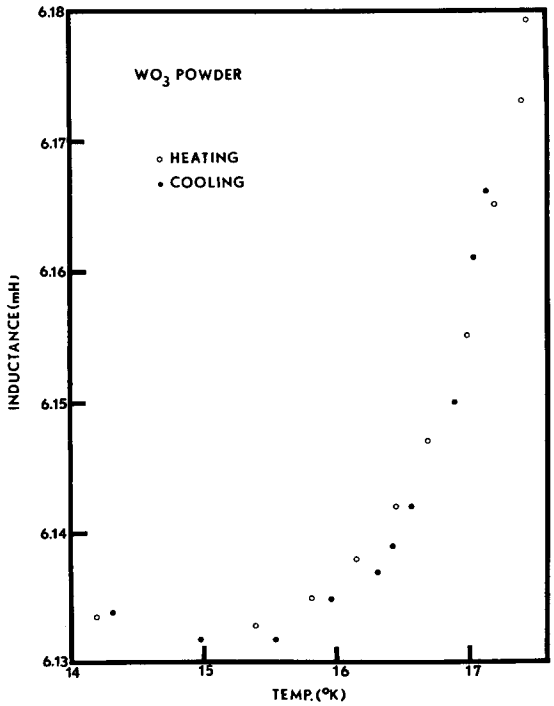


FIG. 6. Inductance of stoichiometric $WO_3$ powder near 15°K.

in the room-temperature phase and all domains had essentially the same orientation in that phase. Resistivity measurements made at moderate heating and cooling rates at temperatures near phase transitions nevertheless show a rather large degree of scatter. This scatter would be expected if phase transitions nucleate independently in different domains, as has sometimes been observed in microscopic studies (*13*, *14*). Scatter can be minimized if slow heating and cooling rates (<0.5°/min) are employed near phase transition temperatures. Plots of log $\rho$ versus $1/T$ yield straight lines for the temperature intervals between phase transitions if these precautions are taken. Values of the activation energy for conduction, calculated from the slopes of these lines in the customary manner (*39*), are listed in Table II. The slope of log $\rho$ versus $1/T$ breaks sharply near 14°K, as log $\rho$ becomes almost independent of temperature. Mutual inductance measurements on packed $WO_3$ powders show a slight decrease of inductance with temperature which gives an inductance minimum at 15.5°K (Fig. 6).

### *B. Oxygen-Deficient Tungsten Trioxide*

Resistivity changes with temperature of a crystal of tungsten trioxide rendered oxygen-deficient by heating it at 1090°K for 36 hr in a vacuum of $10^{-5}$ Torr are shown in Fig. 7. These measurements were made by the four-point probe method, with the points collinear in an arbitrary direction on the (001) face of the crystal. Resistivity increases monotonically with decreasing temperature in a manner typical of nondegenerate semiconductors in the temperature interval 230–300°K. A discontinuous change in resistivity occurs at 260°K. Plots of log $\rho$ versus $1/T$ yield straight lines in the temperature intervals 260–300°K and 230–260°K, the slopes of which yield activation energies for conduction of 0.032 and 0.062 eV, respectively. Small discontinuities and nonlinearities in plots of log $\rho$ versus $1/T$ observed in measurements on some oxygen-deficient tungsten trioxide crystals may be caused by independent nucleation of domains during these resistivity measurements; otherwise, similar results have been obtained using

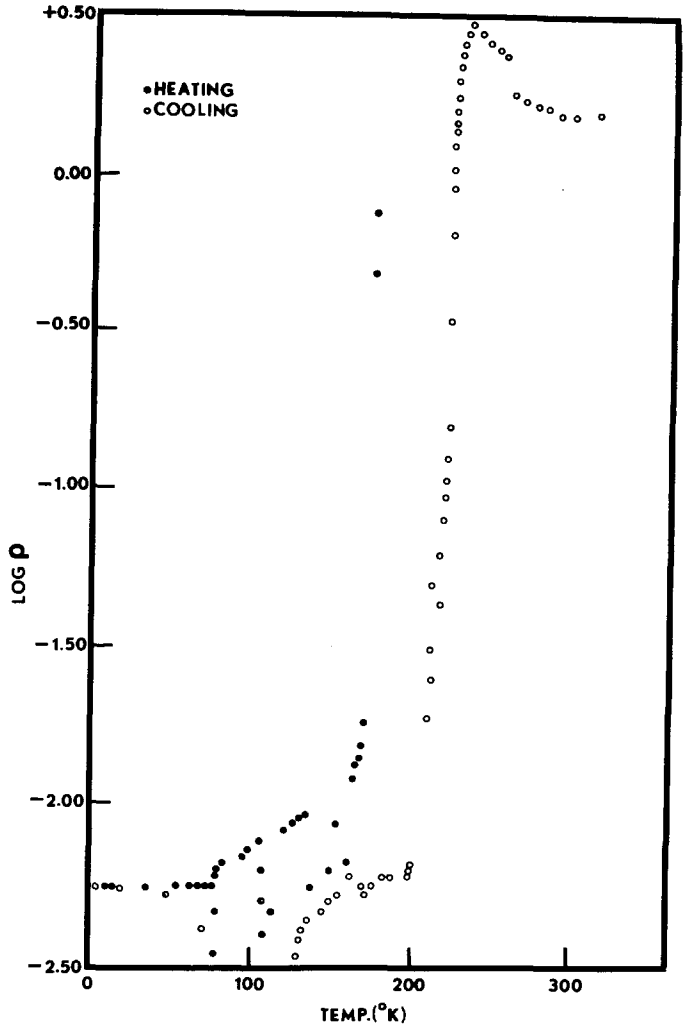


FIG. 7. The ac resistivity of an oxygen-deficient tungsten trioxide crystal prepared by heating a stoichiometric $WO_3$ single crystal at 1090°K *in vacuo* for 36 hr. Anomalies occur near 260, 220, 130, and 80°K. Note the large discontinuity in resistivity and the change in the sign of the temperature coefficient of resistivity at 220°K.

several different crystals. Crystals that exhibit these deviations from linear log $\rho$ versus $1/T$ behavior near phase transitions also exhibit large thermal hysteresis in resistivity values. Plots of log $\rho\, T^{3/2}$ versus $1/T$ yield an energy gap between impurity levels and the conduction band of 0.009 eV in the phase occurring between 220 and 260°K; the energy gap appears to be negligible in the phase occurring at room temperature

A substantial decrease in resistivity occurs in the temperature interval 200–230°K. The temperature coefficient of resistivity is positive in the interval 130–200°K. The magnitude of the resistivity in this temperature interval is appropriate for a degenerate semiconductor, as is the sign of the temperature coefficient of resistivity. Thus, a phase transition from a high-temperature semiconducting phase to a low-temperature metallic phase occurs in the interval 200–230°K, these wide limits being associated with large thermal hysteresis

effects. Resistivity discontinuities also occur near 130°K and near 80°K; the temperature coefficient of resistivity is positive in the interval between these two temperatures also. Resistivity is almost independent of temperature from 4.2 to 80°K.

## 5. Discussion

Capacitance and resistivity anomalies observed in this work occur at definite temperatures or in definite temperature intervals and are clearly associated with phase transformations. Similar phase transitions are observed in stoichiometric and oxygen-deficient tungsten trioxide crystals. Crystal structures of stoichiometric $WO_3$ phases in the temperature interval 130–600°K have been reported previously (*14*), and additional crystallographic information has been presented here. The crystal structure of oxygen-deficient tungsten trioxide at room temperature has been reported (*22, 23*); oscillation X ray diffraction patterns of the room-temperature phase and of the phase occurring in the temperature interval 130–220°K are given in Fig. 2.

### *A. Stoichiometric $WO_3$*

Single crystal X ray (*14*) and neutron diffraction (*33*) studies have shown that a phase of stoichiometric $WO_3$ that occurs in the temperature interval 260–600°K is monoclinic and centrosymmetric, with space group $P2_1/n$ and 8 formula units of $WO_3$ per unit cell. Studies of electron transport properties in this phase have established that the dominant electron scattering process in this phase is longitudinal optic mode scattering (*19*). This scattering process must be considered in polar semiconductors if the static dielectric constant significantly exceeds the optical-frequency dielectric constant given by $\varepsilon \approx n^2$ (*39*). For $WO_3$ at room temperature, $n \approx 2.5$ (*17*). Sienko and Crowder have shown that $WO_3$ single crystals grown by vapor transport on sealed Pt crucible walls have lower Hall mobilities and higher electron effective masses than crystals formed at the same time on a bulk powder charge in the same crucible. They have speculated that crystals grown on platinum lack a center of symmetry, whereas crystals grown on the $WO_3$ powder charge contain one (*19*). Our stoichiometric $WO_3$ single crystals have been grown on platinum. Single crystal X ray photographs show them to lack a center of symmetry and to have a *c*-axis repeat distance of 3.85 Å (Fig. 1a), half that reported by Tanisaki (*14*). Our crystals evidently correspond to the additional room temperature phase suspected by Crowder and Sienko. The additional resistivity contribution from piezoelectric acoustic-mode scattering expected in these crystals is consistent with the suggestion that lower Hall mobilities and higher electron effective masses of vapor-grown crystals are associated with lack of a center of symmetry.

Single-crystal X ray studies of the phase of stoichiometric $WO_3$ that occurs in the temperature interval 220–260°K have established that this phase is triclinic, with 8 formula units per unit cell, and lacks a center of symmetry (*14*). Since this phase is piezoelectric, one might expect acoustic mode contributions to the resistivity. Increases in Hall mobility and thermoelectric power at the 260°K phase transition have been interpreted as phonon-drag contributions caused by such acoustic modes (*6*). Resistivity measurements reported here yield an activation energy for conduction of 0.10 eV in this phase; the same value may be calculated from other data (*6*). While we have not obtained single-crystal X ray patterns in this phase, the coincidence of activation energies for conduction of vapor-deposited $WO_3$ crystals used in this investigation with that of bulk-grown crystals (*6*) indicates that both room-temperature phases transform to the same low-temperature phase, This implies that a doubling of the *c*-axis of vapor-grown crystals occurs at the 260°K phase transition. It is interesting that this *c*-axis doubling does not affect the electrical characteristics of the transition or the transition temperature.

Displacements accompanying the 220°K transition are quite large (*14*) and many crystals crack during thermal cycling through

the phase transition. This phase occurs in the temperature interval 130–220°K. Its most probable structure is monoclinic, with 4 formula units per unit cell, but it may also be indexed as triclinic with 8 formula units per unit cell (*14*). Neither indexing involves a change in unit cell multiplicity in the *c* direction at 220°K. A large increase in thermoelectric power and the disappearance of a Hall voltage in this phase have been attributed to a large phonon drag effect typical of electron scattering in ferroelectrics and in antiferroelectrics (*6*). Resistivity measurements reported here yield an activation energy for conduction of 0.19 eV, consistent with the expectation of a new or additional scattering mechanism in this phase. This activation energy is considerably larger than that which can be calculated from some other resistivity measurements (*6*); However, extremely small deviations from stoichiometry are associated with comparatively large changes in the activation energy for conduction in this phase (*22*, *23*).

The strong temperature dependence of $\varepsilon$ in the (001) direction from 130 to 220°K is consistent with other observations which argue for the existence of ferroelectricity in this phase. The transverse optic mode frequency of a ferroelectric is expected to be strongly temperature-dependent and to vanish at the transition temperature (*11*), this mode makes a dominant contribution to the dielectric constant according to the Lyddane–Sachs–Teller relationship (*40*). While a strongly temperature-dependent dielectric constant is observed in measurements of $\varepsilon$ in the (001) direction of stoichiometric $WO_3$ single crystals, $\varepsilon$ measured in this direction is almost independent of temperature below 130°K. This would be expected if the vanishing of such a *soft* mode below 130°K gave rise to a ferroelectric low-temperature phase. References to ferroelectricity in tungsten trioxide below 220°K (*5*) are based on observations of ferroelectric hysteresis phenomena at 77°K (*5*, *41*). These observations appear to have been made on the phase which occurs from 65 to 130°K.

Capacitance and resistivity anomalies indicate that a structurally distinct phase of tungsten trioxide occurs in the temperature interval 65–130°K. The crystallographic symmetry and lattice parameters of this phase have not been determined. However, capacitance data strongly suggest that the crystallographic symmetry of this phase differs substantially from that of the phase which occurs in the temperature interval 130–220°K. Measurements made in the *c* direction between (001) faces of stoichiometric $WO_3$ single crystals indicate that $\varepsilon$ is almost constant below 130°K, and show furthermore that $\varepsilon \approx n^2$. Thus, strongly anharmonic lattice vibrations do not make a significant contribution to $\varepsilon$ in this direction below 130°K. Measurements made using sintered powder pellets show a strongly temperature-dependent dielectric constant about 10 times larger than that found in the single crystal nominal [001] direction, in apparent good agreement with other measurements of $\varepsilon$ in this temperature region (*5*). Such a sudden loss of a low mode contribution in the *c* direction of $WO_3$ would be expected if the soft mode of the phase occurring from 130 to 220°K were associated with the multiplicity of the *c* parameter in that phase, and if the soft mode and attendant unit cell multiplicity were absent in the phase occurring from 65 to 130°K.

The accumulated evidence seems to show that there is no ferroelectric polarization along the *c*-axis from 65 to 130°K. The dielectric constant and tan $\delta$ of single crystals are both independent of temperature as would be expected if no anharmonic polar distortions occurred in this direction; indeed, the observation that $\varepsilon \approx n^2$ shows that no such distortions can be present. Furthermore, bulk volume resistivity measurements in this phase yield an activation energy for conduction of 0.052 eV, compared with 0.19 eV in the phase occurring from 130 to 220°K. Such a large decrease in the activation energy would be consistent with the loss, in this phase, of a scattering process occurring in the higher temperature phase.

It appears quite likely, however, that ferroelectric displacements occur in either the *a* or *b* directions of this phase. Hysteresis loops have been observed in pressed pellets

of stoichiometric $WO_3$ powder at 77°K in the present work, as well as in previous accounts (*5*, *41*). Similar hysteresis loops have been observed in single crystals of unspecified orientation (*42*). However, it appears that none of these loops has indicated complete saturation polarization. It would not be surprising to observe unsaturated loops in measurements on pressed powder pellets, for such powders tend to pack with the (001) planes of easy cleavage horizontal. This will favor contributions from the relatively nonpolar *c* direction. It is possible that out present failure to observe hysteresis loops on nominal (111) faces of $WO_3$, and the apparent failure of others (*42*) to obtain complete saturation in measurements on single crystals, may result from a rigid crystal or domain structure, which would *clamp* the polarization reversal. Similar clamping effects have been seen during measurements on sodium niobate (*15*, *16*). Observation of a tan $\delta$ maximum in measurements on pressed powders at 130°K would also be consistent with the existence of a ferroelectric low-temperature phase. If a change in unit cell multiplicity in fact accompanies a polar distortion at 130°K, as suggested here, the strong analogy between phase transitions in $WO_3$ and $NaNbO_3$ may be worthy of note (*1*, *43*). An antiferroelectric phase of $NaNbO_3$ having 4 formula units per unit cell transforms to a ferroelectric phase, the unit cell of which contains only 2 formula units (*15*, *16*).

A variety of observations indicates that the phase which occurs between 40 and 65°K is more symmetrical than the phase which occurs from 65 to 130°K. Capacitance measurements on stoichiometric $WO_3$ pressed powder pellets and on single crystals exhibit small thermal hysteresis at the 65°K transition. These observations, and observations of resistivity discontinuities in stoichiometric $WO_3$ near 65°K, demonstrate that this is a displacive transition. The dielectric constant measured in the *c* direction is constant in this temperature interval, with $\varepsilon \approx n^2$. Measurements on pressed $WO_3$ powder pellets show that $\varepsilon$ decreases by about a factor of 2 in this 25° interval. This temperature dependence of $\varepsilon$ is smaller than in phases which occur at a higher temperature and suggests that the contribution to $\varepsilon$ of temperature-dependent vibrational modes has become less important. Electrical resistivity data are in accord with this suggestion. The activation energy for conduction of 0.028 eV observed in this phase is about half that of the phase occurring above 65°K, and would be consistent with loss of a phonon drag contribution from a ferroelectric phase occurring above 65°K.

Tan $\delta$ and $\varepsilon$ are essentially independent of temperature in the phase that occurs below 40°K. Measurements of $\varepsilon$ parallel to the *c* direction on $WO_3$ single crystals show $\varepsilon = 10$, while measurements on pressed powders yield $\varepsilon = 20$. This phase appears to have a markedly anisotropic crystal structure, but there is no indication that this structure would be susceptible to significant distortion in an electric field.

A variety of electronic phenomena indicate the existence of some transition near 15°K. A rather sharp break in the slope of $\log \rho$ versus $1/T$ at this temperature, together with the slight inductance minimum shown in Fig. 6, may be typical of low-temperature effects that have been attributed to the interaction of impurity bands with the conduction bands of polar semiconductors (*44*). It is a novel feature of this transition that after some critical field is applied, large currents may sometimes be obtained without arc breakdown of the crystal. Since the use of a megohmmeter to measure the extremely large resistance encountered in this temperature region involves the application of rather large potentials near the surface of the crystal, the conditions required for the observation of this phenomenon are not clearly defined. This electronic transition does not appear to involve a structural change.

### *B. Oxygen-Deficient Tungsten Trioxide*

An X ray diffraction investigation has established that the room-temperature phase of oxygen-deficient tungsten trioxide crystals is related to that of vapor-grown stoichiometric $WO_3$ single crystals by a doubling of the *c* parameter, while the phase of oxygen-

deficient tungsten trioxide which occurs from 130 to 220°K appears to have a structure identical to that of stoichiometric $WO_3$. Measurements of electrical resistivity as a function of temperature have shown discontinuities at 260, 220, 130, and 80°K. These temperatures are quite close to those that mark phase transitions in stoichiometric $WO_3$ crystals, and it appears that phase transitions occur in oxygen-deficient tungsten trioxide at all these temperatures except possibly the last. However, it is especially interesting that the sign of the temperature coefficient of resistivity of oxygen-deficient tungsten trioxide differs from that of stoichiometric $WO_3$ in all these phases except the one occurring from 220 to 260°K. Berak and Sienko have already noted that activation energies for conduction decrease in magnitude with increase in oxygen deficiency in the temperature interval 110–290°K while activation energies for conduction increase in magnitude with increase in oxygen deficiency in the room temperature phase (*22*, *23*). They suggest that the observed resistivity of oxygen-deficient crystals can be resolved into two contributions: (1) New scattering processes in the oxygen-deficient shear plane regions; and (2) the scattering processes discussed previously, which continue to operate in the essentially stoichiometric *host* $WO_3$ lattice. The demonstration here that all phases of oxygen-deficient tungsten trioxide except the one occurring from 220 to 260°K have a temperature coefficient of resistivity opposite in sign to that of the corresponding stoichiometric phase is entirely consistent with this suggestion. Indeed, such a superposition of resistivity mechanisms may account for failure to observe the monoclinic-to-triclinic phase transition near 290°K and the displacive transition near 220°K in some compositions of oxygen-deficient tungsten trioxide (*22*, *23*).

Studies of the lattice dynamics of oxygen-deficient tungsten trioxide in the monoclinic room-temperature phase and in the triclinic phase occurring from 220 to 260°K are complicated by the apparent similarities between the conduction mechanisms of the oxygen-deficient shear-plane regions and the essentially stoichiometric host crystal. Both materials are extrinsic semiconductors in both phases, and their contributions to the observed conductivity are comparable. The resistivity of oxygen-deficient tungsten trioxide in the phase occurring below 220°K is so much lower than that of stoichiometric $WO_3$, however, that resistivity measurements in this phase must reflect primarily the electrical transport properties of oxygen-deficient shear plane regions. The change from a negative temperature coefficient of resistance above 220°K to a positive temperature coefficient of resistance below that temperature, and the discontinuous decrease in resistivity at that temperature, establish the metallic (or highly degenerate semiconductor) character of this phase. This strong temperature-dependence of resistivity would be expected if electron scattering occurs primarily by interaction with lattice modes. These lattice modes would be likely to include polar acoustic modes as well as the optic modes encountered in the room-temperature phase. In view of the observed structural similarities between stoichiometric $WO_3$ and nonstoichiometric tungsten trioxide at 200°K (Figs. 1 and 2) it would not be surprising to find electron scattering due to lattice modes in the phase of tungsten trioxide occurring below 220°K. It is possible that semiconductor-to-metal phase transitions are characteristic of oxygen-deficient shear structures related to tungsten trioxide; Berak and Sienko have found a broad semiconductor-to-metal phase transition as $WO_{2.895}$ (slightly oxygen-deficient $W_{20}O_{58}$) is cooled below 270°K (*22*, *23*).

The resistivity discontinuity occurring near 130°K in oxygen-deficient tungsten trioxide may possibly reflect the phase transition of the host stoichiometric $WO_3$ lattice and need not involve a structural rearrangement of the oxygen-deficient shear planes. The temperature coefficient of resistivity does not change sign at this resistivity discontinuity, although it appears to decrease somewhat in magnitude. A constant residual resistivity is observed below 80°K; it is therefore not certain whether a phase transition occurs at this temperature.

## Acknowledgment

We gratefully acknowledge the many helpful suggestions of M. J. Sienko.

## References

1. S. Sawada, *J. Phys. Soc. Japan* **11**, 1237, 1246 (1956).
2. R. Ueda and T. Ichinokawa, *Phys. Rev.* **82**, 563 (1951).
3. S. Sawada, R. Ando, and S. Nomura, *Phys. Rev.* **82**, 952 (1951).
4. W. L. Kehl, R. G. Hay, and D. Wahl, *J. Appl. Phys.* **23**, 212 (1952).
5. B. T. Matthias, *Phys. Rev.* **76**, 430 (1949).
6. B. L. Crowder and M. J. Sienko, *Inorg. Chem.* **4**, 73 (1965).
7. I. Lefkowitz, M. A. Shields, G. Dolling, W. J. L. Buyers, and R. A. Cowley, *J. Phys. Soc. Japan, Suppl.* **28**, 249 (1970).
8. S. Hoshino, K. Shimaoka, N. Nimura, H. Moteg, and N. Maruyama, *J. Phys. Soc. Japan, Suppl.* **28**, 189 (1970).
9. E. Hanamura, *J. Phys. Soc. Japan, Suppl.* **28**, 192 (1970).
10. P. W. Anderson, in "Proceedings of the International Conference on Dielectrics," Moscow (1958).
11. W. Cochran, *Adv. Phys.* **9**, 387 (1960); **18**, 157 (1969).
12. A. A. Maradudin, E. W. Montroll, and G. H. Weiss, *in* "Solid State Physics" (F. W. Seitz and D. Turnbull, Eds.), Suppl. 3, p. 1, Academic Press, New York (1963).
13. K. Hirakawa, *J. Phys. Soc. Japan* **7**, 331 (1952).
14. S. Tanisaki, *J. Phys. Soc. Japan* **15**, 566, 573 (1960).
15. I. Lefkowitz, K. Lucaszewicz, and H. D. Megaw, *Acta Cryst.* **20**, 670 (1966).
16. I. Lefkowitz, Ph.D. Thesis, Cambridge Univ. (1963).
17. S. Sawada and G. C. Danielson, *Phys. Rev.* **113**, 1005, 1008 (1959).
18. B. Wanklyn, *J. Crystal Growth* **2**, 251 (1968).
19. B. L. Crowder and M. J. Sienko, *J. Chem. Phys.* **38**, 1576 (1963).
20. R. LeBihan and C. Vacherand, *in* "Croissance de composes Minéraux Monocristallins" (J. P. Suchet, Ed.), p. 147, Masson et cie, Paris (1969).
21. E. Gebert and R. J. Ackermann, *Inorg. Chem.* **5**, 136 (1966).
22. J. M. Berak and M. J. Sienko, *J. Solid State Chem.* **2**, 109 (1970).
23. M. J. Sienko and J. M. Berak, *in* "The Chemistry of Extended Defects in Non-Metallic Solids," p. 541, North-Holland, Amsterdam (1970).
24. R. J. D. Tilley, *Mater. Res. Bull.* **5**, 813 (1970).
25. C. W. Chu, *Phys. Rev.* **1B**, 4700 (1970).
26. S. Tanisaki, *J. Phys. Soc. Japan* **11**, 620 (1956).
27. G. Meyer, J. F. Oosterom, and J. L. De Roo, *Rec. Trav. Chim.* **78**, 412 (1959).
28. C. B. Alcock and G. W. Hooper, *Proc. Roy. Soc. Ser. A.* **254**, 551 (1960).
29. H. Schäfer and A. Tebben, *Z. Anorg. Allgem. Chem.* **304**, 317 (1960).
30. R. Ueda and T. Ichinokawa, *Phys. Rev.* **80**, 1106 (1950).
31. R. Ueda and J. Kobayashi, *Phys. Rev.* **91**, 1565 (1953).
32. G. Anderson, *Acta Chem. Scand.* **7**, 154 (1953).
33. E. O. Loopstra and P. Boldrini, *Acta Cryst.* **21**, 158 (1966).
34. H. Bräkken, *Z. Krist.* **78**, 484 (1931).
35. J. A. Perri, E. Banks, and B. Post, *J. Appl. Phys.* **28**, 1272 (1957).
36. W. Kleber, M. Hännert, and R. Müller, *Z. Anorg. Allgem. Chem.* **346**, 113 (1966).
37. W. L. Pillinger, P. S. Jastram, and J. G. Daunt, *Rev. Sci. Instr.* **29**, 159 (1958).
38. P. Chieux, Ph.D. Thesis, Cornell Univ., 1969; Diss. Abstr. **31**, 1198B (1970); Mich. Univ. Microfilms, Ann Arbor, No. 70–14, 375.
39. A. R. Hutson, *in* "Semiconductors" (N. B. Hannay, Ed.), p. 541, Reinhold, New York (1959).
40. R. H. Lyddane, R. G. Sachs, and E. Teller, *Phys. Rev.* **59**, 673 (1941).
41. B. T. Matthias and E. A. Wood, *Phys. Rev.* **84**, 1255 (1951).
42. R. LeBihan and C. Vacherand, *J. Phys. Soc. Japan, Suppl.* **28**, 159 (1970).
43. H. D. Megaw, "Ferroelectricity in Crystals," Methuen, London (1957).
44. E. H. Putley, "The Hall Effect and Related Phenomena," p. 161, Butterworths, London (1960).